

## Lectin Biosensing Using Digital Analysis of Ru(II)-Glycodendrimers

Raghavendra Kikkeri, Dan Grünstein, and Peter H. Seeberger\*

Department of Biomolecular Systems, Max Planck Institute of Colloids and Interfaces, Am Mühlenberg 1, 14476 Potsdam, Germany, and Institute of Chemistry and Biochemistry, Free University Berlin, Arnimallee 22, 14195 Berlin, Germany

Received May 5, 2010; E-mail: peter.seeberger@mpikg.mpg.de

**Abstract:** A novel, digital, single-operation analytical method to study glycodendrimer–lectin interactions is described. Robust, highly fluorescent derivatives of tris(bipyridine)ruthenium(II) ( $[\text{Ru}(\text{bipy})_3]^{2+}$ ) bearing 2, 4, 6, or 18 mannose or galactose units were designed to perform molecular logic operations. Inputs for these systems were pH, *N,N'*-4,4'-bis(benzyl-2-boronic acid)bipyridinium dibromide, and different lectins (concanavalin A, *Galantus nivalis* agglutinin, and asialoglycoprotein). The relative change in fluorescence quantum yield of the Ru(II)-glycodendrimers served as output. Together, the fluorescent emission readout, the logic analysis of the photoinduced electron transfer, and the optical behavior provide a single-step method to quickly screen a glycodendrimer library and select the best dendrimer model for studying carbohydrate–lectin interactions.

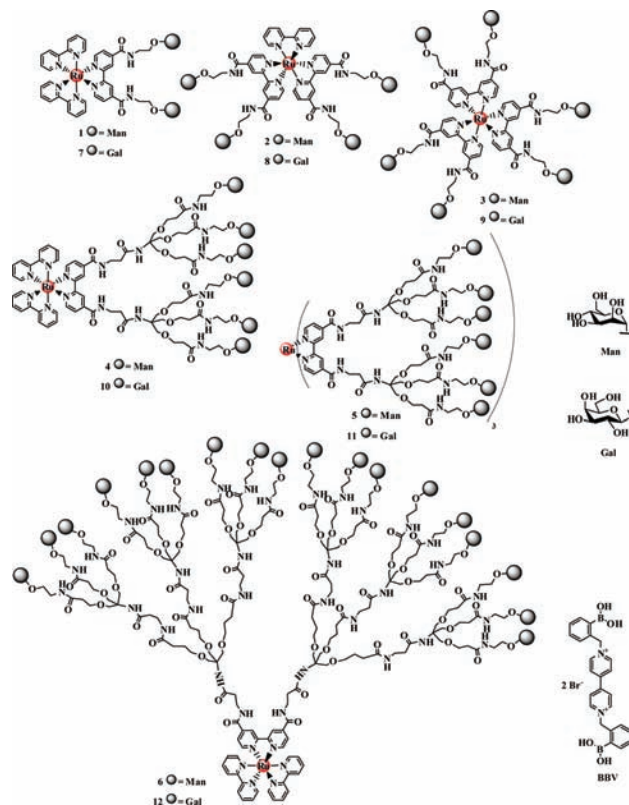
Logic gates perform basic logical functions using one or more inputs of binary values and produce a single output of 0 or 1 (false or true). Molecular logic gates involve similar principles and use a chemical or biological process as input and spectroscopic emissions as the output signal. Different molecules such as DNA, proteins, carbohydrates, and metals have been used as active components of molecular logic gates.<sup>1</sup> However, until now, carbohydrate–protein interactions have not been utilized as the basis for logic operations, even though the utility of such a tool would be widespread. Carbohydrates play a crucial role in many important biological processes involving cellular recognition, including cell adhesion, migration, apoptosis, and trafficking.<sup>2</sup> However, the binding affinities of individual carbohydrates for carbohydrate-binding proteins (lectins) are typically quite weak; hence, multivalent carbohydrate–protein interactions are often employed by nature to achieve tight binding. To this end, a variety of multivalent structures have been synthesized to display carbohydrates, including a fluorescent complex and a template-based structure.<sup>3</sup> Glycodendrimers are an important example of these synthetic molecules, because they can mimic cell surface glycan arrays and can be used as optical and electrochemical probes to sense lectins when they are complexed onto a tris(bipyridine)ruthenium(II) ( $[\text{Ru}(\text{bipy})_3]^{2+}$ ) derivative.<sup>4</sup> To fully harness the potential of glycodendrimers as a screening tool, we have developed a molecular logic gate-based method to analyze the various properties of different glycodendrimers that influence specific carbohydrate–protein interactions. In contrast to established screening methods, which require an extensive instrumental setup and technical expertise,<sup>5</sup> molecular logic gates provide a straightforward and conceptually different approach based on a clear-cut binary output to analyze changes in properties. Here, we present molecular logic operations based on the analysis of a collection of mannose- or galactose-decorated glycodendrimers with a fluorescent Ru(II) core during the photoinduced electron transfer (PET) and the optical behavior that occur during the lectin sensing process. This technology provides a single-

step method to screen a collection of glycodendrimers and determine the best dendrimer model for studying carbohydrate–lectin interactions.

The glycodendrimer collection (1–12) is comprised of 12 robust, highly fluorescent and synthetically accessible glycodendrimers, each with a Ru(II) core, bearing 2, 4, 6, or 18 carbohydrate units of mannose or galactose (Scheme 1). Each glycodendrimer was used as the active component to perform logic operations with defined chemical inputs: pH, BBV, and lectin. Concanavalin A (ConA) and *Galantus nivalis* agglutinin (GNA), which recognize mannose, and asialoglycoprotein (ASGPR), which interacts with galactose, were selected as lectins. The optical readout from the PET lectin sensor is generated by displacement of *N,N'*-4,4'-bis(benzyl-2-boronic acid)bipyridinium dibromide (BBV) from the glycodendrimer sugar array by lectins. This results in a relative change in fluorescent quantum yield of the Ru(II)-glycodendrimers.

Complexes 1–3 and 7–9 were prepared starting from 4,4'-dicarboxyl-2,2'-bipyridine. The carboxylic acid was activated with thionyl chloride and treated with 2'-aminoethyl mannoside or galactoside to yield 13 or 14. Bipyridine ligands 13 and 14 were treated with  $[\text{Ru}(\text{bipy})_2]\text{Cl}_2$  or  $\text{RuCl}_3$  in ethanol, and finally deacetylation with

**Scheme 1.** Structures of Ru(II)-glycodendrimers 1–12



sodium methoxide afforded complexes **1** and **7**, or **2** and **8**, or **3** and **9** (see Supporting Information (SI), section 2). Ru(II)-glycodendrimers **4–6** and **10–12** were prepared as described previously.<sup>4</sup>

Logic gate analysis of electron transfer between complexes **1–12** and BBV displayed two different outputs with BBV and pH 7.4 as inputs. Complexes **1–4** displayed effective electron transfer resulting in NAND logic gates. NAND logic is represented by the situation where the output, in this case the relative quantum fluorescence yield, is quenched or FALSE (0) only when both inputs (pH and BBV) are TRUE (1,1) (the threshold for a TRUE response was set at 0.45) (Figure 1). In contrast, the output for complexes **5** and **6** was TRUE (1) even for the (1,1) input showing tautology. The differences in the relative quantum yield for complexes **1–6** must be related to the different density of dendritic encapsulation. Since the boronic acids have high sugar affinities, all complexes bind to BBV at pH 7.4.<sup>6</sup> However, differences in the density and distribution of the carbohydrate that encapsulates the Ru(II) core result in different degrees of fluorescence quenching, inducing different quantum yields (see SI, Table S1). Fluorescence quenching is much greater for complexes **1–4**, indicating that the high degree of carbohydrate density in complexes **5** and **6** prevents electron transfer to BBV since the Ru(II) core is more protected by the topology of the hydrophilic core of sugars than in complexes **1–4**. A similar behavior was observed with complexes **7–12** (see SI, Figure S3).

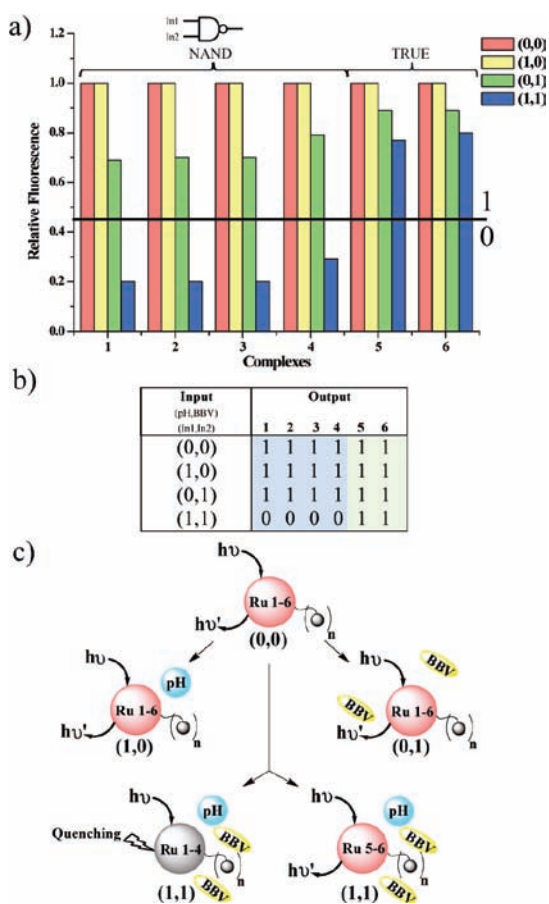


**Figure 1.** (a) Schematic representation of relative fluorescence responses to pH and BBV as inputs: concn of complexes **1–6**,  $0.5 \times 10^{-5}$  M; concn of BBV,  $25.0 \times 10^{-5}$  M; pH 7.4 in phosphate buffer. (b) Corresponding truth table. (c) Schematic diagram of the mechanism of interaction.

After investigating the PET between the Ru(II) core and BBV, we focused on the effect that lectin binding had upon the fluorescent output. For complexes **1–3**, with ConA and buffer (pH) as inputs,

the logic operations rendered FALSE output (contradiction), indicating no binding with lectin (Figure 2). However, with the same inputs, complexes **4–6** performed as AND gates (Figure 2). In the AND logic, a high output (1) or increase in quantum yield results only if both inputs to the AND gate are high (1). If neither, or only one input to the AND gate is high, a low (0) output results. Since carbohydrate–protein interactions are quite weak, and complexes **1–3** are decorated with relatively few sugars, ConA binding resulted in only a small change in fluorescence. However, the larger dendrimers **4–6** interacted more effectively with ConA and showed an increase in the fluorescent signal due to aggregation and encapsulation of the Ru(II) core by the carbohydrates and the resulting more hydrophilic environment of the protein. By setting 1.15 as the threshold level, complexes **4–6** exhibited AND logic and are therefore the best system to study lectin–carbohydrate interactions in the fluorescent mode. In contrast, ConA does not bind galactose, and, as expected, complexes **7–12** produce only FALSE output (see SI, Figure S6). Similar experiments with the higher valency mannose-binding lectin GNA were performed, and the same overall effect was observed. The opposite outcome was obtained when using ASGPR, which binds galactose. Complexes **1–6**, which contain mannose, and the sparsely decorated complexes **7–9** displayed contradiction (FALSE output), whereas components **10–12** with a high number of galactose units behaved as AND gates (see SI, Figures S7–S10).

After gaining insight into how the logic operation helps in the straightforward analysis of the PET and the optical lectin sensing process affected by dendrimer structures, we studied how complexes

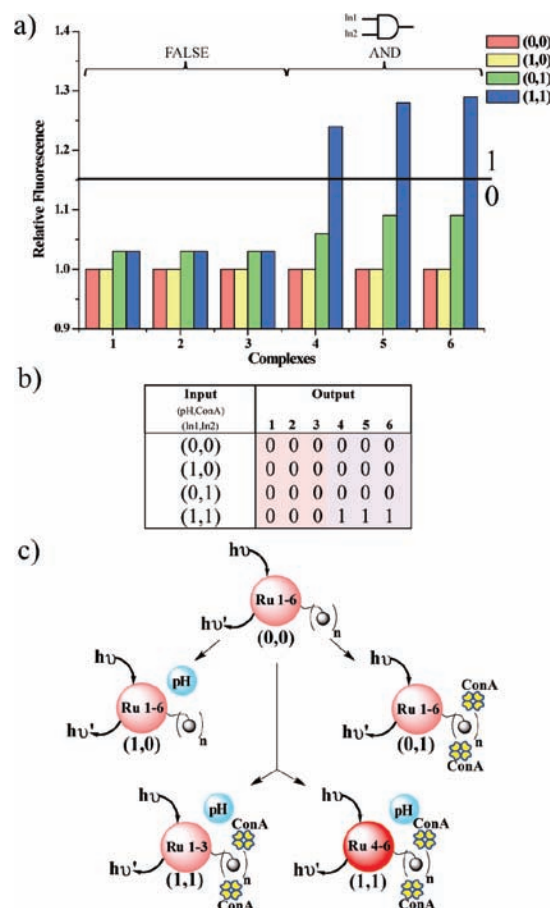


**Figure 2.** (a) Schematic representation of relative fluorescence responses to pH and ConA as inputs: concn of complexes **1–6**,  $0.5 \times 10^{-5}$  M; concn of ConA,  $1.0 \times 10^{-6}$  M; pH 7.4 in phosphate buffer with 0.1 mM  $\text{CaCl}_2$  and 0.1 mM NaCl. (b) Corresponding truth table. (c) Schematic diagram of the mechanism of interaction.

1–12 behave over three inputs (pH, BBV, and lectin). Three-input study will give an opportunity to identify the best model of selective and sensitive lectin sensors. To exclude the effects of nonspecific carbohydrate–lectin interactions, we set the threshold level at 1.15 (Figure 3). Complexes 1–3 showed FALSE output due to weaker carbohydrate–lectin interactions and high PET quenching with BBV. Complexes 5 and 6 resulted in an AND gate with no significant influence of BBV due to weak quenching with the electron acceptor. Consequently, complexes 5 and 6 are better suited for optical lectin sensing than PET. However, a three-input INHIBIT gate was successfully constructed with complex 4 by combining the molecular input components of the NAND and AND gates. An INHIBIT gate represents a situation where a high third input (BBV) inhibits the output of a gate that previously behaved as an AND gate independent of the other two inputs.<sup>7</sup> To achieve this, the structure of 4 must allow for the perfect balance of lectin binding and PET. This is evident when, with all three inputs present, the optical readout of 4 is compared with those of complexes 1–3 (smaller structures with fewer sugar units), in which 4 demonstrates a comparative increase in fluorescence due to effective displacement of BBV by ConA (Figure 3). In similar experiments with GNA and ASGPR, only complexes 4 and 10 acted as INHIBIT gates, respectively (see SI, Figures S12 and S13). Finally, using best model 4, ConA and GNA lectins were detected at the limit range of 25–28 nM,<sup>4a</sup> and by using complex 10, ASGPR could be sensed at 38 nM (see SI, Figure S14).

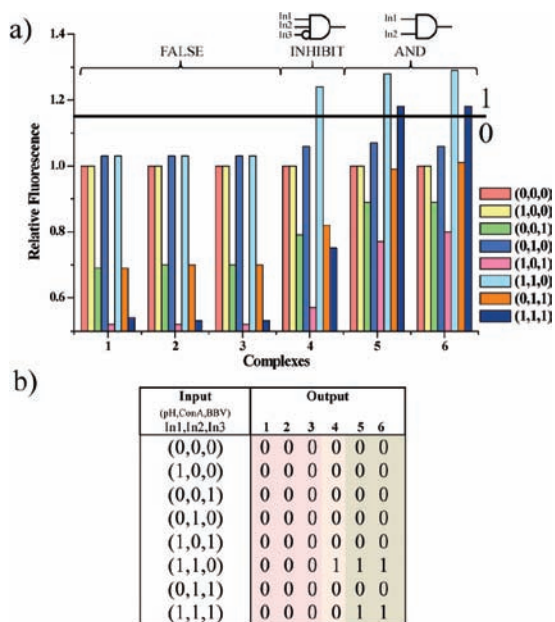


**Figure 3.** (a) Schematic representation of relative fluorescence responses to pH and ConA as inputs: concn of complexes 1–6,  $0.5 \times 10^{-5}$  M; concn of ConA,  $1.0 \times 10^{-6}$  M; concn of BBV,  $25.0 \times 10^{-5}$  M; pH 7.4 in phosphate buffer with 0.1 mM  $\text{CaCl}_2$  and 0.1 mM NaCl. (b) Corresponding truth table.

In conclusion, a novel, digital, single-operation analytical method to study glycodendrimer–lectin interactions is described. Using this binary system, glycodendrimers were found to behave in two different modes. Complexes 1–3 constitute a NAND gate based on effective PET but failed to display lectin binding. In contrast, complexes 5 and 6 bind well to lectin (and thus behave as AND gates) but due to higher sugar density, only weak PET was observed. Complex 4 exhibited a perfect balance between both processes and thus is presented as an effective INHIBIT gate. This demonstrates that a Ru(II)-glycodendrimer exhibiting six mannoses is the best to sense ConA or GNA lectins, and similarly complex 10 (with six galactoses) performs best

when screening for ASGPR lectin binding. Thus, by using logic operations, it is possible to generalize the real-time straightforward analysis of biological interactions and the sensing process.

**Acknowledgment.** We thank the Max-Planck Society and the European Union FP7 (CARMUSYS) for financial support.

**Supporting Information Available:** Full experimental details for synthesis of metal dendrimers and optical studies. This material is available free of charge via the Internet at <http://pubs.acs.org>.

## References

- (a) de Silva, A. P.; Uchiyama, S. *Nat. Nanotechnol.* **2007**, *2*, 399–410. (b) Desilva, A. P.; Gunaratne, H. Q. N.; McCoy, C. P. *Nature* **1993**, *364*, 42–44. (c) Margulies, D.; Melman, G.; Shanzler, A. *Nat. Mater.* **2005**, *4*, 768–771. (d) Ashkenasy, G.; Ghadiri, M. R. *J. Am. Chem. Soc.* **2004**, *126*, 11140–11141. (e) Baron, R.; Lioubashevski, O.; Katz, E.; Niazov, T.; Willner, I. *J. Phys. Chem. A* **2006**, *110*, 8548–8553. (f) Margulies, D.; Felder, C. E.; Melman, G.; Shanzler, A. *J. Am. Chem. Soc.* **2007**, *129*, 347–354. (g) Margulies, D.; Hamilton, A. D. *J. Am. Chem. Soc.* **2009**, *131*, 9142–9143. (h) Zhou, J.; Melman, G.; Pita, M.; Ornatka, M.; Wang, X. M.; Melman, A.; Katz, E. *ChemBiochem* **2009**, *10*, 1084–1090. (i) Niazov, T.; Baron, R.; Katz, E.; Lioubashevski, O.; Willner, I. *Proc. Natl. Acad. Sci. U.S.A.* **2006**, *103*, 17160–17163. (j) De Silva, A. P.; James, M. R.; McKinney, B. O. F.; Pears, D. A.; Weir, S. M. *Nat. Mater.* **2006**, *5*, 787–790. (k) Gupta, T.; van der Boom, M. E. *Angew. Chem., Int. Ed.* **2008**, *47*, 2260–2262. (l) Gianneschi, N. C.; Ghadiri, M. R. *Angew. Chem., Int. Ed.* **2007**, *46*, 3955–3958. (m) Credi, A.; Balzani, V.; Langford, S. J.; Stoddart, J. F. *J. Am. Chem. Soc.* **1997**, *119*, 2679–2681. (n) Frezza, B. M.; Cockroft, S. L.; Ghadiri, M. R. *J. Am. Chem. Soc.* **2007**, *129*, 14875–14879.
- (a) Drickamer, K.; Taylor, M. E. *Annu. Rev. Cell Biol.* **1993**, *9*, 237–264. (b) Liu, F. T. *Clin. Immunol.* **2000**, *97*, 79–88. (c) Konstantinov, K. N.; Robbins, B. A.; Liu, F. T. *Am. J. Pathol.* **1996**, *148*, 25–30. (d) Pilobello, K. T.; Slawek, D. E.; Mahal, L. K. *Proc. Natl. Acad. Sci. U.S.A.* **2007**, *104*, 11534–9. (e) Bertozzi, C. R.; Kiessling, L. L. *Science* **2001**, *291*, 2357–2364. (f) Lis, H.; Sharon, N. *Chem. Rev.* **1998**, *98*, 637–674.
- (a) Metullio, L.; Ferrone, M.; Coslanich, A.; Fuchs, S.; Fermeglia, M.; Paneni, M. S.; Priel, S. *Biomacromolecules* **2004**, *5*, 1371–1378. (b) de Paz, J. L.; Noti, C.; Bohm, F.; Werner, S.; Seeberger, P. H. *Chem. Biol.* **2007**, *14*, 879–887. (c) Andre, J. P.; Galdes, C.; Martins, J. A.; Merbach, A. E.; Prata, M. I. M.; Santos, A. C.; de Lima, J. P.; Toth, E. *Chem.–Eur. J.* **2004**, *10*, 5804–5816. (d) Benito, J. M.; Gomez-Garcia, M.; Mellet, C. O.; Baussanne, I.; Defaye, J.; Fernandez, J. M. *G. J. Am. Chem. Soc.* **2004**, *126*, 10355–10363. (e) Turnbull, W. B.; Kalovidouris, S. A.; Stoddart, J. F. *Chem.–Eur. J.* **2002**, *8*, 2988–3000. (f) Ashton, P. R.; Boyd, S. E.; Brown, C. L.; Negogodiev, S. A.; Meijer, E. W.; Peeringling, H. W. I.; Stoddart, J. F. *Chem.–Eur. J.* **1997**, *3*, 974–984. (g) Kikkeri, R.; Hossain, L. H.; Seeberger, P. H. *Chem. Commun.* **2008**, 2127–2129. (h) Huang, C. C.; Chen, C. T.; Shiang, Y. C.; Lin, Z. H.; Chang, H. T. *Anal. Chem.* **2009**, *81*, 875–882. (i) Gao, J. Q.; Liu, D. J.; Wang, Z. X. *Anal. Chem.* **2008**, *80*, 8822–8827. (j) Chabre, Y. M.; Roy, R. *Adv. Carbohydr. Chem. Biochem.* **2010**, *63*, 165–393.
- (a) Kikkeri, R.; Garcia-Rubio, I.; Seeberger, P. H. *Chem. Commun.* **2009**, 235–237. (b) Kikkeri, R.; Kamena, F.; Gupta, T.; Hossain, L. H.; Boonyarattanakalin, S.; Gorodyska, G.; Beurer, E.; Coullerez, G.; Textor, M.; Seeberger, P. H. *Langmuir* **2010**, *26*, 1520–1523. (c) Ibey, B. L.; Beier, H. T.; Rounds, R. M.; Cote, G. L.; Yadavalli, V. K.; Pishko, M. V. *Anal. Chem.* **2005**, *77*, 7039–7046. (d) Krist, P.; Vannucci, L.; Kuzma, M.; Man, P.; Sadalapure, K.; Patel, A.; Bezouska, K.; Pospisil, M.; Petrus, L.; Lindhorst, T. K.; Kren, V. *ChemBiochem* **2004**, *5*, 445–452. (e) Okada, T.; Makino, T.; Minoura, N. *Bioconjugate Chem.* **2009**, *20*, 1296–1298. (f) Hasegawa, T.; Yonemura, T.; Matsuura, K.; Kobayashi, K. *Bioconjugate Chem.* **2003**, *14*, 728–737. (g) Hasegawa, T.; Yonemura, T.; Matsuura, K.; Kobayashi, K. *Tetrahedron Lett.* **2001**, *42*, 3989–3992. (h) Kikkeri, R.; Liu, X. Y.; Adibekian, A.; Tsai, Y. H.; Seeberger, P. H. *Chem. Commun.* **2010**, *46*, 2197–2199. (i) Gottschaldt, M.; Schubert, U. S.; Rau, S.; Yeno, S.; Vos, J. G.; Kroll, T.; Clement, J.; Hilger, I. *ChemBioChem* **2010**, *11*, 649.
- (a) Horlacher, T.; Seeberger, P. H. *Chem. Soc. Rev.* **2008**, *37*, 1414–1422. (b) Chen, S. M.; LaRoche, T.; Hamelinck, D.; Bergsma, D.; Brenner, D.; Simeone, D.; Brand, R. E.; Haab, B. B. *Nat. Methods* **2007**, *4*, 437–444. (c) Chen, S.; Haab, B. B. *Clin. Prot.* **2008**, *101*–111. (d) Lekka, M.; Laidler, P.; Labedz, M.; Kulik, A. J.; Lekki, J.; Zajac, W.; Stachura, Z. *Chem. Biol.* **2006**, *13*, 505–512. (e) Dai, Z.; Kawde, A. N.; Xiang, Y.; La Belle, J. T.; Gerlach, J.; Bhavanandan, V. P.; Joshi, L.; Wang, J. *J. Am. Chem. Soc.* **2006**, *128*, 10018–10019.
- (a) Suri, J. T.; Cordes, D. B.; Cappuccio, F. E.; Wessling, R. A.; Singaram, B. *Angew. Chem., Int. Ed.* **2003**, *42*, 5857–5859. (b) Cordes, D. B.; Gamsay, S.; Sharrett, Z.; Miller, A.; Thoniyot, P.; Wessling, R. A.; Singaram, B. *Langmuir* **2005**, *21*, 6540–6547.
- (a) Saghatelian, A.; Volcker, N. H.; Guckian, K. M.; Lin, V. S. Y.; Ghadiri, M. R. *J. Am. Chem. Soc.* **2003**, *125*, 346–347. (b) de Silva, A. P.; Dixon, I. M.; Gunaratne, H. Q. N.; Gunlaugsson, T.; Maxwell, P. R. S.; Rice, T. E. *J. Am. Chem. Soc.* **1999**, *121*, 1393–1394. (c) Cheah, I. K.; Langford, S. J.; Latter, M. J. *Supramol. Chem.* **2005**, *17*, 121–128.

JA103688S